

Provided for non-commercial research and education use.  
Not for reproduction, distribution or commercial use.



This article appeared in a journal published by Elsevier. The attached copy is furnished to the author for internal non-commercial research and education use, including for instruction at the authors institution and sharing with colleagues.

Other uses, including reproduction and distribution, or selling or licensing copies, or posting to personal, institutional or third party websites are prohibited.

In most cases authors are permitted to post their version of the article (e.g. in Word or Tex form) to their personal website or institutional repository. Authors requiring further information regarding Elsevier's archiving and manuscript policies are encouraged to visit:

<http://www.elsevier.com/copyright>



Contents lists available at ScienceDirect

Applied Surface Science

journal homepage: [www.elsevier.com/locate/apsusc](http://www.elsevier.com/locate/apsusc)

## Effect of swift heavy ion irradiation in Fe/W multilayer structures

Sharmistha Bagchi<sup>a,\*</sup>, Shahid Anwar<sup>b</sup>, N.P. Lalla<sup>a</sup>

<sup>a</sup> UGC-DAE Consortiums for Scientific Research, Khandwa Road, Indore 452001, India

<sup>b</sup> Central Electro Chemical Research Institute (CECRI), Karaikudi 630006, India

### ARTICLE INFO

#### Article history:

Available online 14 August 2009

#### Keywords:

Fe/W MLS  
Swift heavy ion irradiation  
X-TEM  
WAXD  
Magnetic measurement

### ABSTRACT

Present study reports effect of swift heavy ion irradiation on structural and magnetic properties of sputtered Fe/W multilayer structures (MLS) having bilayer compositions of [Fe(20 Å)/W(10 Å)]<sub>5BL</sub> and [Fe(20 Å)/W(30 Å)]<sub>5BL</sub>. These MLS are irradiated by 120 MeV Au<sup>9+</sup> ions up to fluence of  $4 \times 10^{13}$  ions/cm<sup>2</sup>. X-ray reflectivity (XRR), wide-angle X-ray diffraction (WAXD), cross-sectional transmission electron microscopy (X-TEM) and magneto optical Kerr effect (MOKE) techniques are used for structural and magnetic characterization of pristine and irradiated MLS. Analysis of XRR data using Parratt's formalism shows a significant increase in W/Fe interface roughness. WAXD and X-TEM studies reveals that intra-layer microstructure of Fe-layers in MLS becomes nano-crystalline on irradiation. MOKE study shows increase in coercivity at higher fluence, which may be due to increase in surface and interface roughness after recrystallization of Fe-layers.

© 2009 Elsevier B.V. All rights reserved.

### 1. Introduction

Tailoring the properties of functional materials at atomic scale, these days is an ultimate research goal in material science. In this context, layer-by-layer growth is the most desirable method to fabricate structures with atomic precision, artificially. Ability to control thin film growth, layer-by-layer, has advanced our understandings of physics and physical phenomena like Giant Magneto Resistance (GMR) in two-dimensional systems. This is reported for magnetic metallic combinations like Fe/Cr, Co/Cu, Fe/Mo, W/Fe [1–6], which found a tremendous impact in GMR and magnetic data storage. However, in these systems interface quality plays a decisive role to achieve optimum performance of GMR applications [7,8].

Swift heavy ions (SHI) lose their energy via inelastic collisions and lead to electronic excitation in target material. This electronic energy loss found to induce various modifications including creation of defects, intermixing and alloy formation [9–12]. Material modification using SHI has been studied in metals [9] as well as in insulators [13]. Particularly in metals, where damage creation occurs when electronic energy loss exceeds a certain threshold value [14]. Effects of SHI, different in bulk and thin films [15,16], have been explained using two models, thermal spike model [17] and ion-explosion model [18]. Electron mediated sputtering yield is enhance in Au films and is dependent on film

thickness [19]. Recently we have reported nearly immiscible stable superlattice MLS in W/Ni [20]. Application of W based immiscible multilayer structure is promising for technological applications [20,21].

Therefore we report here effect of swift heavy ion irradiation on Fe/W multilayer structure to study, its stability under SHI. Such studies are expected to throw light on the mechanism of material modification due to electronic energy loss.

### 2. Experimental

Fe/W multilayers with five bilayer structure of [Fe(20 Å)/W(10 Å)] and [Fe(20 Å)/W(30 Å)] on silicon [1 0 0] substrate were deposited employing ion-beam sputtering at base pressure of  $1 \times 10^{-7}$  Torr and during deposition the pressure was maintained at  $4 \times 10^{-4}$  Torr [22]. Here after MLS [Fe(20 Å)/W(10 Å)]<sub>5BL</sub> and [Fe(20 Å)/W(30 Å)]<sub>5BL</sub> on silicon will be referred as FeW10 and FeW30. The coated substrates were cut into 10 mm × 10 mm pieces and subjected to 120 MeV Au<sup>9+</sup> ions irradiated at room temperature up to fluence of  $4 \times 10^{13}$  ions/cm<sup>2</sup>. Irradiation was performed using 15UD Pelletron accelerator at IUAC, New Delhi.

Pristine and irradiated MLS were characterized through X-ray reflectivity (XRR) and wide-angle X-ray diffraction (WAXD) using  $\theta$ - $2\theta$  diffractometer configured in symmetrical Bragg–Brentano geometry mounted on a rotating anode (Cu-K $\alpha$ ) X-ray generator. For detail microstructural characterization, cross-sectional TEM (X-TEM) studies were carried out, using Tecnai-G<sup>2</sup>-20 TEM operating at 200 kV. X-TEM samples were prepared following the standard technique [20]. Final thinning of the sample was done

\* Corresponding author at: UGC-DAE Consortiums for Scientific Research, Khandwa Road, Indore 452001, India. Tel.: +91 731 2463913; fax: +91 731 2462294.  
E-mail address: [bagchi.sharmistha@gmail.com](mailto:bagchi.sharmistha@gmail.com) (S. Bagchi).

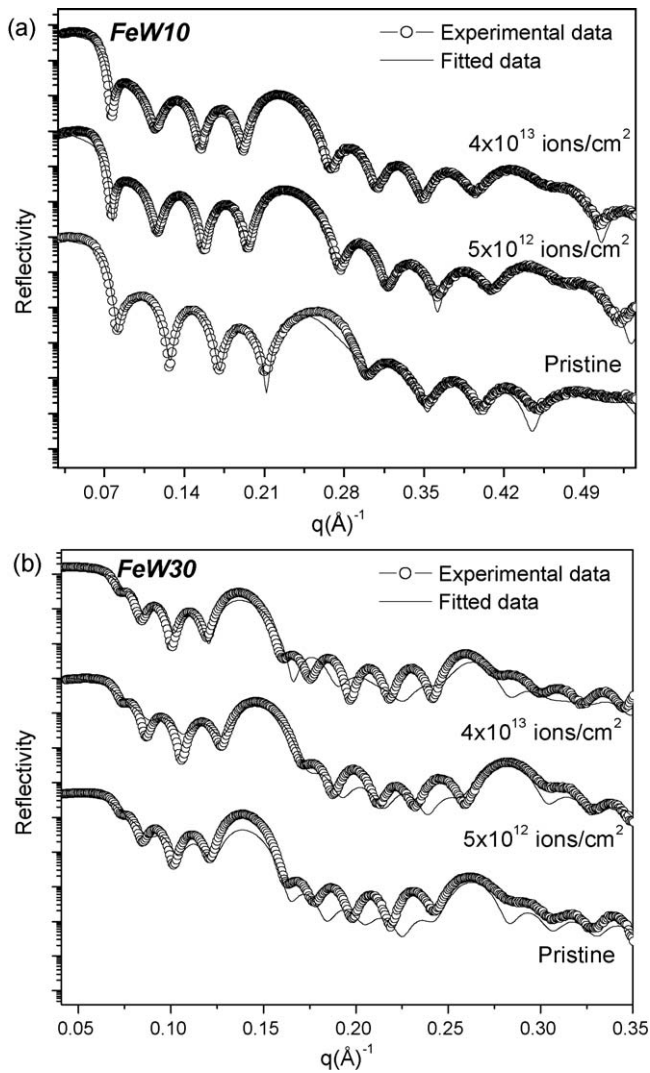


**Fig. 1.** X-ray reflectivity patterns of the pristine and irradiated multilayer structure of (a) *FeW10* and (b) *FeW30*. The XRR patterns corresponding to different fluences are shifted for clarity.

using Ar ion-beam polishing at 3 kV/20  $\mu$ A at grazing incidence of 3°. Magnetic behaviors of the MLS were studied at each stage of irradiation using magneto optical Kerr effect (MOKE). MOKE measurements were performed in longitudinal mode, using He–Ne laser source of 6328 Å wavelengths.

### 3. Results

#### 3.1. X-ray reflectivity study

Fig. 1a and b shows a comparative XRR pattern of pristine as well as SHI irradiated Fe/W multilayers. From the comparative plot one can clearly see the presence of Bragg peaks and kissig fringes, which indicate a good quality of deposited MLS. These XRR patterns were fitted using Parratt's formalism to estimate layer thickness and interface roughness [23]. Refined fit parameters are listed in Table 1. The presence of Bragg peaks up to second order in the irradiated MLS; signify that SHI is not destroying the structural arrangement of multilayer. The structure is remains intact after SHI. Normally these types of feature direct us that the systems are immiscible. So on the basis of observed XRR data clearly shows that the deposited Fe/W system is immiscible on subjected to SHI [5]. Refined parameters from Table 1 indicate that there is an increase

**Table 1**  
The values of fit parameters, like layer thickness and interface roughness of *FeW10* and *FeW30* obtained using "Parratt's formalism".

Sample name/irradiated dose	Layer thickness (Å)		Interface roughness (Å)	
	W	Fe	W	Fe
<i>FeW10</i>				
Pristine	10	20	4	5
$5 \times 10^{12}$ ions/cm <sup>2</sup>	8	19	5	5
$4 \times 10^{13}$ ions/cm <sup>2</sup>	9	18	7	9
<i>FeW30</i>				
Pristine	31	19	5	5
$5 \times 10^{12}$ ions/cm <sup>2</sup>	30	17	5.5	5
$4 \times 10^{13}$ ions/cm <sup>2</sup>	29	16	8	9.5

in interface roughness as a function of irradiation fluence from ~5 Å to ~9 Å.

Further, it can be noted, that there is a shift in Bragg peak position in irradiated MLS with respect to pristine samples. The observed shift is mainly due to variation of layer thicknesses in different regions (10 mm  $\times$  10 mm) of large substrate (50 mm  $\times$  50 mm) used for deposition.

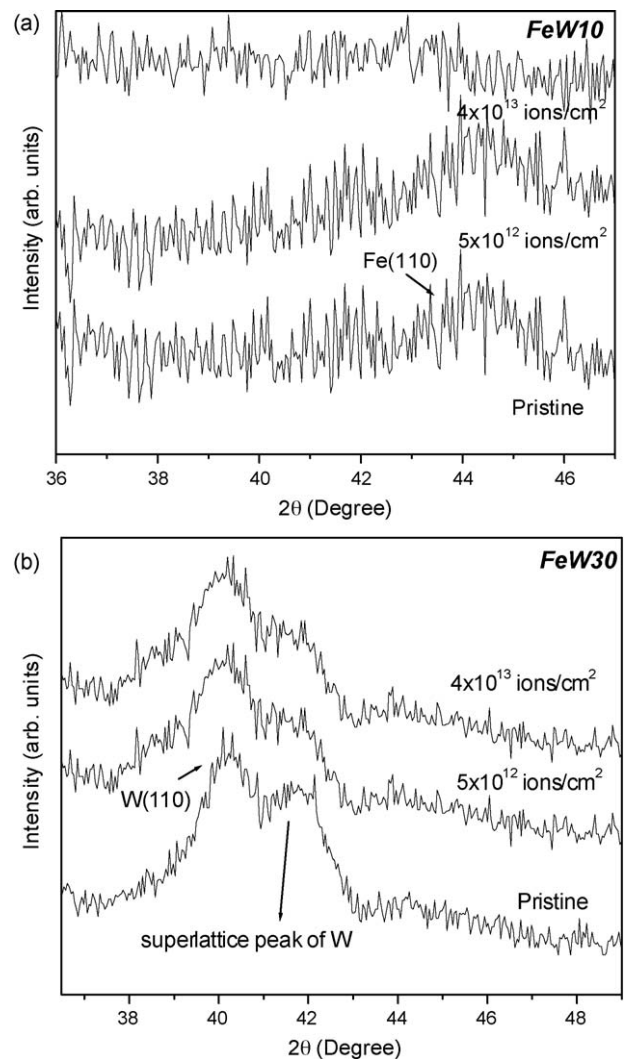


**Fig. 2.** Wide-angle X-ray diffraction patterns of pristine as well as irradiated (a) *FeW10* and (b) *FeW30* multilayer structures. The patterns corresponding to different irradiation doses are shifted for clarity.

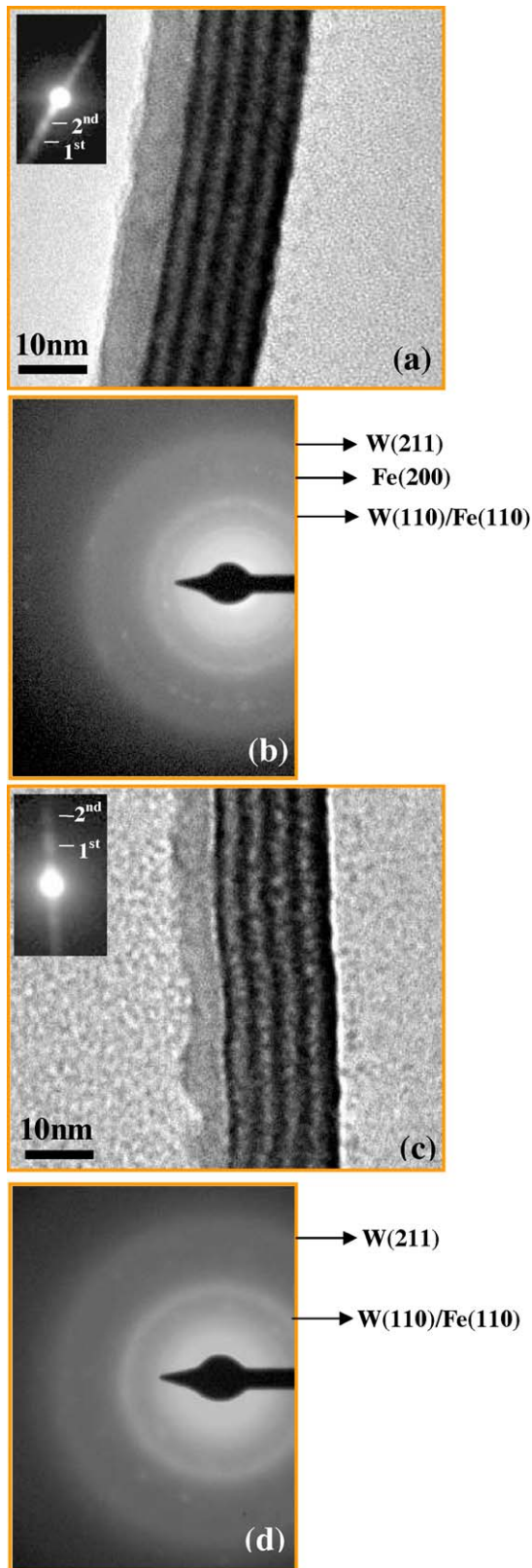


**Fig. 3.** Cross-sectional TEM micrographs of (a) pristine and (c)  $4 \times 10^{13}$  ions/cm<sup>2</sup> irradiated *FeW10* multilayers. The corresponding SAD patterns are shown in (b) and (d) respectively. (a) The black and white strips correspond to W- and Fe-layers respectively. Inset shows the corresponding low-angle SAD patterns. The micrograph in (c) shows irradiation-induced nano-crystallization of each Fe-layer without any intermixing of W and Fe. In the SAD pattern (b) shows the polycrystalline growth of Fe/W MLS. The continuous and broad diffraction rings of the SAD in (d) reveal the random aggregation of nano-crystalline Fe.

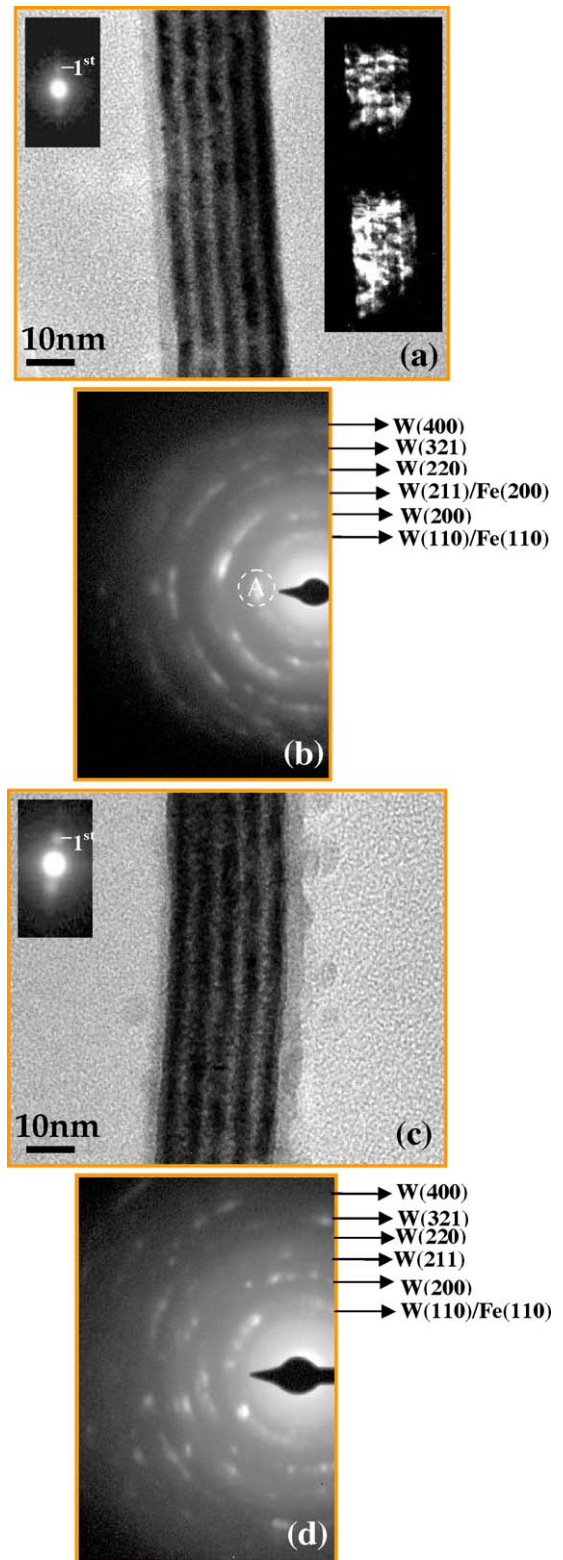


**Fig. 4.** Cross-sectional TEM micrographs of (a) pristine and (c)  $4 \times 10^{13}$  ions/cm<sup>2</sup> irradiated *FeW30* multilayers. The corresponding SAD patterns are shown in (b) and (d) respectively. Left Inset and right inset shows the corresponding low-angle SAD and dark field patterns respectively. The micrograph in (c) shows irradiation-induced nano-crystallization of Fe-layers. SAD pattern of (b) shows the intense (1 1 0) reflection indicate [1 1 0] textured growth of the W-layers. This textured is not perfect throughout the multilayers as the presence of W(2 0 0), W(2 1 1), W(2 2 0), W(3 2 1) and W(4 0 0) grain orientation too. The continuous and broad diffraction ring of Fe along with [1 1 0] textured structure of the W in the SAD in (d) reveal the random aggregation of nano-crystalline Fe.

### 3.2. Wide-angle X-ray diffraction study

WAXD patterns of pristine and irradiated *FeW10* MLS (Fig. 2a) indicate weak diffraction maxima of  $\text{Fe}(1\ 1\ 0)$ , which nearly vanishes after irradiation up to fluence of  $4 \times 10^{13}$  ions/cm<sup>2</sup>. This suggests that there is a decrease in structural order of Fe-layers in *FeW10* MLS or system is moving towards more nano-crystallization or there is an increase nano-crystallization in Fe-layers. However, the absence of diffraction peak due to W in pristine MLS suggests that W-layers are either amorphous or nano-crystalline with very weak diffracted intensity.

In the case of pristine and irradiated *FeW30* MLS (Fig. 2b) indicate Peak at  $41.27^\circ$  adjacent to  $\text{W}(1\ 1\ 0)$  peak. Superlattice peak appearing in WAXD pattern may be correlated with textured growth of W along  $[1\ 1\ 0]$  direction. In addition, superlattice growth of W along  $[1\ 1\ 0]$  is not affected due to irradiation up to higher fluence of  $4 \times 10^{13}$  ions/cm<sup>2</sup>. The absence or very weak diffraction peak due to Fe suggests amorphous or nano-crystalline growth of Fe-layers in *FeW30* MLS [5]. The position of the diffraction peaks do not exactly correspond to the positions already known for thick films or bulk materials published in ICDD database, that may be due to reduce third dimension of thin films.

### 3.3. Transmission electron microscopy study

X-TEM investigations were carried out in imaging and selected area diffraction (SAD) modes on pristine and  $4 \times 10^{13}$  ions/cm<sup>2</sup> irradiated samples of *FeW10* and *FeW30* MLS.

X-TEM micrograph in (Fig. 3a) alternate black and white layers (Z-contrast of W and Fe) occurring periodically at  $\sim 30\ \text{\AA}$  [21,22]. One can see the presence of intense Bragg spots (inset of Fig. 3a) of low-angle SAD indicative of coherence in pristine MLS. Similar microstructural and low-angle SAD (inset of Fig. 4a) features can be seen for the pristine *FeW30* MLS with a periodicity of  $\sim 50\ \text{\AA}$  (Fig. 4a). These micrographs show growth of Fe- and W-layers with rough interface, similar to XRR see Table 1. SAD taken from *FeW10* MLS is shown in Fig. 3b. Continuous diffraction rings in Fig. 3b shows a polycrystalline growth of Fe and W grains in corresponding layers. Unlike *FeW10* MLS, SAD (Fig. 4b) taken from *FeW30* shows the presence of discontinuous diffraction rings with rather intense spots which is due to textured growth of  $\text{W}(1\ 1\ 0)$  layers. To further confirm this texturing, dark field (DF) image was (right inset in Fig. 4a) taken from  $(1\ 1\ 0)$  spot of W (A) (Fig. 4b) indicates columnar textured growth of  $\text{W}(1\ 1\ 0)$ , similar kind of textured behavior also observed in WAXD patterns. However, this texturing of W-layers is not perfect throughout, due to the presence of feeble rings of  $\text{W}(2\ 0\ 0)$ ,  $\text{W}(2\ 1\ 1)$ ,  $\text{W}(2\ 2\ 0)$ ,  $\text{W}(3\ 2\ 1)$  and  $\text{W}(4\ 0\ 0)$ . Thus, polycrystalline structure can be inferred from a strong textured inside and partly random grain orientation outside of columns.

Microstructural and diffraction data (Figs. 3c and 4c) corresponding to irradiated samples show different features as compared to pristine samples. Although interfaces are intact for both MLS, intra-layer contrast of Fe-layers has changed to nano-crystalline aggregate after irradiation. Recrystallization of MLS has caused coarsening of Fe-layers, which in turn further increases interface roughness [20,21]. This increased interface roughnesses were already being cleared from fitting of XRR data as shown in Table 1. Black and white Z-contrast still seen even in irradiated MLS depicts that SHI has been able to cause coarsening of grains in Fe-layers. As already proposed by WAXD, X-TEM investigation further conformed that the Fe/W interface is still unmixed. Occurrence of continuous but broad diffraction ring of  $\text{Fe}(1\ 1\ 0)$  (Fig. 3d) exhibits nano-crystalline aggregate of Fe-layers. Unchanged SAD pattern of W with nano-crystalline Fe-ring after SHI is shown in Fig. 4d. Pristine W-layers remain be unaffected because melting point of W is very large 3695 K [24].

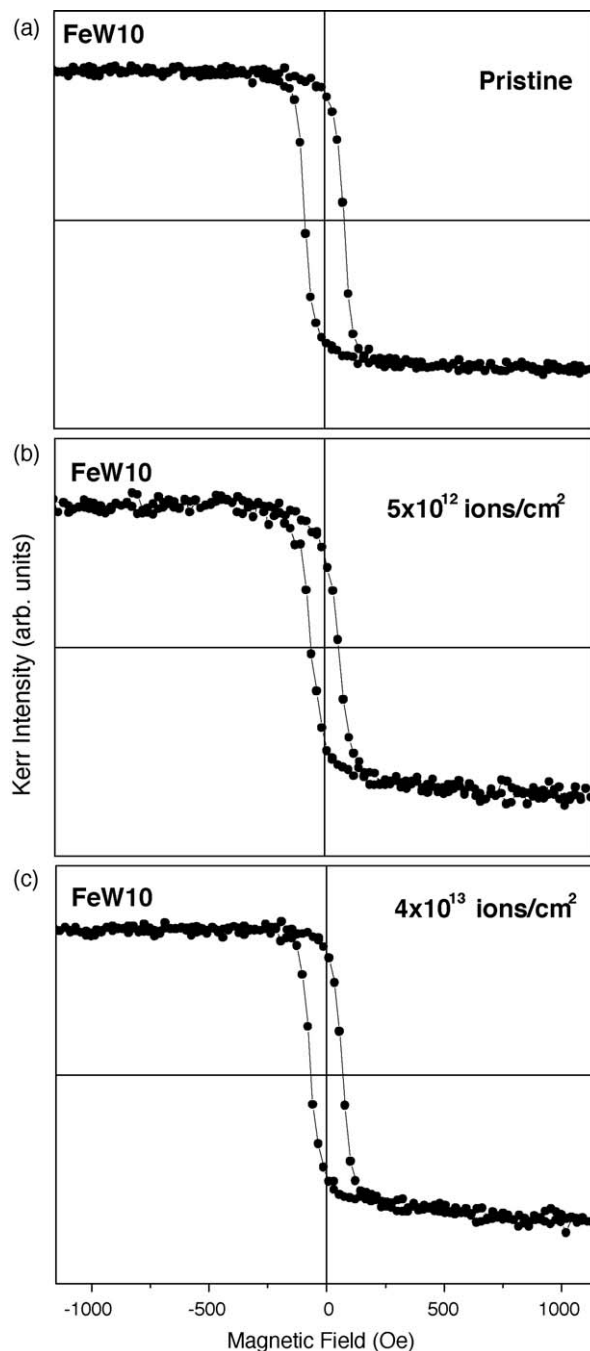


Fig. 5. Shows the hysteresis loops of (a) pristine (b)  $5 \times 10^{12}$  ions/cm<sup>2</sup> and (c)  $4 \times 10^{13}$  ions/cm<sup>2</sup> *FeW10* MLS samples.

### 3.4. MOKE study

The hysteresis loops were recorded at room temperature by measuring the Kerr rotation (MOKE) with the field applied in the plane of the sample. The MOKE pattern is shown in Figs. 5 and 6.

MOKE measurements on pristine and irradiated *FeW10* (Fig. 5a) and *FeW30* (Fig. 6a) represent a well-defined saturation as a function of applied field. Coercive fields ( $H_c$ ) of 82 Oe (*FeW10*) and 132 Oe (*FeW30*) are determined for pristine MLS. MOKE data for MLS irradiated at  $5 \times 10^{12}$  ions/cm<sup>2</sup> fluence (Figs. 5b and 6b) shows  $H_c$  of 59 Oe (*FeW10*) and 42 Oe (*FeW30*). For MLS irradiated to  $4 \times 10^{13}$  ions/cm<sup>2</sup> (Figs. 5c and 6c) corresponding  $H_c$  are 68 Oe (*FeW10*) and 101 Oe (*FeW30*) as estimated from MOKE hysteresis loops. In both the two MLS of *FeW10* and *FeW30*, it has been

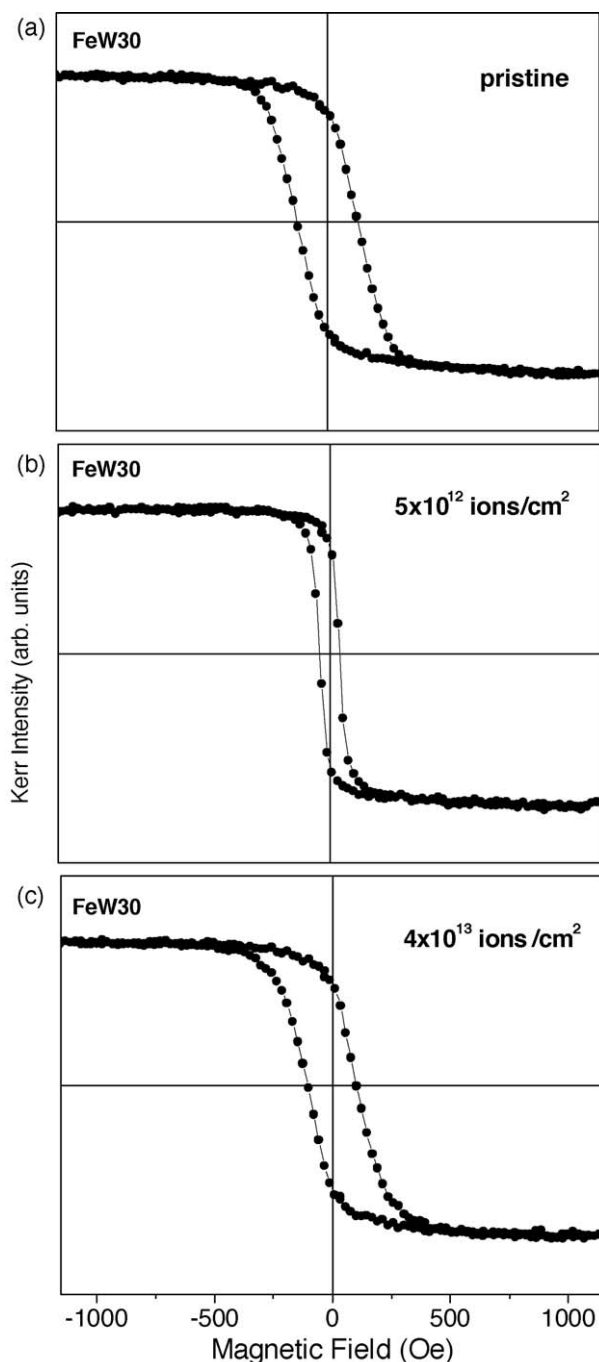


Fig. 6. Show the hysteresis loops of (a) pristine (b)  $5 \times 10^{12}$  ions/cm<sup>2</sup> and (c)  $4 \times 10^{13}$  ions/cm<sup>2</sup> FeW30 MLS samples.

observed that  $H_c$  values decreases first and increases later, as a function of irradiation dose.

#### 4. Discussions

RRR, WAXD, X-TEM and MOKE results of W/Fe MLS of FeW10 and FeW30 indicate difference in interlayer and intra-layer mixing effects of 120 MeV Au<sup>9+</sup> ions. This has been supported by cross-sectional TEM micrographs of irradiated MLS.

In a given target SHI losses its energy mainly through two processes, namely electronic ( $S_e$ ) and nuclear ( $S_n$ ) losses. Swift heavy ions, such as 120 MeV Au<sup>9+</sup> losses most of its energy through electronic excitation process. Using SRIM [25] we could calculate  $S_e$

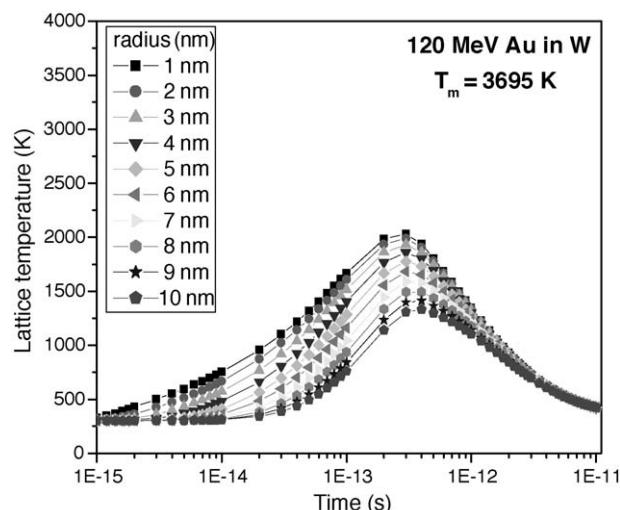


Fig. 7. The evolution of lattice temperature with time in 120 MeV Au ion irradiated on W calculated by the thermal spike model.  $T_m$  is the melting temperature of the metals.

for W/Fe MLS to be 40.4 KeV/nm  $S_e$  for W and 34 KeV/nm for Fe. Similarly, calculated  $S_n$  found to be 1.04 KeV/nm for W and 0.6 KeV/nm for Fe. The consequence of large energy density deposition in material has been described by Coulomb explosion and Thermal spike models. The Coulomb explosion in present case is ruled out due to extremely high plasmon frequency of metallic systems where the electron returns back to the ion core before the occurrence of explosion. Typical Coulomb explosion time being  $10^{-14}$  s and the plasmon frequency being  $10^{15}$  Hz. In the framework of thermal spike model, the energy of electronic subsystem is transferred to the lattice subsystem via electron–phonon coupling [26–28]. These are described by two coupled differential equations, incorporating specific heat and thermal conductivity of the electronic and lattice subsystems [28,29]. Recently Gupta et al. [29] reported computer simulation of temperature rise of a thermal spike generated with the same 120 MeV Au<sup>9+</sup> ions at room temperature in Fe bulk. They have shown that the Fe undergoes transiently molten state for a radius of 2 nm. Plot of temperature rise in W bulk is shown in Fig. 7. The calculation is performed considering the physical parameters of the bulk metal. W still not reach molten state due to large difference between the spike temperature and its melting point. It is evident that Fe undergoes molten state transiently whereas the spike temperature in W does not reach the molten state. The fact that Fe goes to molten state transiently, it may either mix with the material adjacent to it or it will reorganize itself minimizing its energy during recrystallization. It is known that the, heat of mixing of W and Fe is 0 kJ/mole [30,5], therefore no intermixing will take place in Fe/W multilayer during ion irradiation. Therefore no mixing takes place and Fe reorganizes itself as nano-crystallites as shown in X-TEM micrograph of Figs. 3c and 4c.

Irradiations does affect the magnetic properties of MLS. In our case, at a lower fluence the nature of the loop becomes magnetically soft as clearly seen from the decreasing trends in coercivity (Figs. 5b and 6b) [31]. A decrease in coercivity is mainly due to decrease in grain size. This decrease in grain size make the Fe-layers magnetically soft yielding to a lower coercivity. However there is no clear signature of decrease in grain size was detected in WAXD pattern. But MOKE is a very sensitive tool for determining the magnetic properties of the thin films. It will give information of particular area where laser beam is falling. The MOKE information is highly accurate for a particular local area. The small change in

grain size observed in MOKE may not be observable in WAXD. Hence on irradiation very fine grains were developed, which is below the detection limit of WAXD in this case (as peak is already broad and peak height to background ratio is not large), but it is giving a clear signature in MOKE measurements [31,32]. Hysteresis loop corresponding to higher fluence shows increasing trend of  $H_c$  as compared to lower dose irradiated MLS. Here the dominating factor is roughness, i.e., interlayer roughness as well as roughness of individual layer [33–35]. The change in interlayer roughness can be directly compared from Table 1. From Table 1 it is clearly indicated that there is no significant change in roughness for pristine and  $5 \times 10^{12}$  ions/cm<sup>2</sup> irradiated MLS, but a drastic change was observed on comparing pristine and higher dose sample. This increased roughness of both the MLS was also confirmed thorough X-TEM micrographs. It is well establish in MOKE measurement that surface and interface roughness will increase the coercivity. Irradiation also effect the grain size of the system at higher dose system stabilized in nano-crystalline structures, but the dominant factor for reducing coercivity is roughness only. In the bright field image of both MLS, the top layer is Fe, so after irradiation one can clearly identify more rough surface due to recrystallization in Fe-layers.

## 5. Conclusion

Based on above-described structural, microstructural and MOKE studies on pristine and swift heavy ion irradiated Fe/W multilayer structures, the following conclusions have been drawn. Irradiation causes recrystallization of individual Fe-layers, i.e., reduces the correlation length (reduces particle size). Whereas due to immiscible nature of Fe/W multilayer structure, the interface have been found remains intact after irradiation. TEM results do confirm occurrence of nano-crystalline microstructure of individual Fe-layers of swift heavy ion irradiated Fe/W multilayer. MOKE study shows, increase in coercivity at higher fluence due to increased in surface and interface roughness after recrystallization in Fe-layers.

## Acknowledgements

Authors would like to acknowledge Dr. P. Chaddah, prof. A. Gupta for encouragements. We are thankful to Dr. V.R. Reddy for MOKE measurements. Authors thank F. Singh and D.K. Avasthi for their help during irradiation of samples at IUAC New Delhi. Authors are also thankful to S. Potdar for his help during deposition of the

multilayer samples. One of the author (S.B.) would like to acknowledge CSIR New Delhi for financial support.

## References

- [1] C. Dufour, C. Jaouen, G. Marchal, J. Pacaud, J. Grilhe, J.C. Jousset, *J. Appl. Phys.* 81 (1997) 116.
- [2] J. Teillet, F. Richomme, A. Fnidiki, M. Toulemonde, *Phys. Rev. B* 55 (1997) 11560.
- [3] W.Y. Lai, C.Y. Pan, Y.Z. Wang, M.L. Yan, S.X. Li, C.T. Yu, *J. Magn. Mater.* 155 (1996) 358.
- [4] M.L. Yan, D.J. Sellmyer, W.Y. Lai, *J. Phys. Condens. Matter* 9 (1991) L145.
- [5] E. Majkova, S. Luby, M. Jergel, A. Anopchenko, Y. Chushkin, G. Barucca, A. Cristoforo, P. Mengucci, E.D. Anna, A. Luches, M. Martino, H.Y. Lee, *Mater. Sci. Eng. C* 19 (2002) 139.
- [6] E. Majkova, S. Luby, M. Jergel, Y. Chushkin, E.D. Anna, A. Luches, M. Martino, P. Mengucci, G. Majni, Y. Kuwasawa, S. Okayasu, *Appl. Surf. Sci.* 208 (2003) 394.
- [7] D. Srinivasan, S. Sanyal, R. Corderman, P.R. Subramanian, *Metall. Mater. Trans. A* 37A (2006) 995.
- [8] C. Rumbolz, W. Bolse, S. Kumar, R.S. Chauhan, D. Kabiraj, D.K. Avasthi, *Nucl. Instrum. Methods B* 245 (2006) 145.
- [9] A. Iwase, S. Sasaki, T. Iwata, T. Nihira, *Phys. Rev. Lett.* 58 (1987) 2450.
- [10] Ph. Bauer, C. Dufour, C. Jaouen, G. Marchal, J. Pacaud, J. Grilhe, J. Jousset, *J. Appl. Phys.* 81 (1997) 116.
- [11] F. Thibaudau, J. Cousty, E. Balanzat, S. Bou, *Phys. Rev. Lett.* 67 (1991) 1582.
- [12] D. Bhattacharya, G. Principi, A. Gupta, D.K. Avasthi, *Nucl. Instrum. Methods B* 244 (2006) 198.
- [13] R.L. Fleischer, P.B. Brice, R.M. Walker, *J. Appl. Phys.* 36 (1965) 2645.
- [14] A. Gupta, *Vacuum* 58 (2000) 16.
- [15] C. Dufour, Ph. Bauer, G. Marchal, J. Grilhe, C. Jaouen, J. Pacaud, J.C. Jousset, *Europhys. Lett.* 21 (1993) 671.
- [16] P. Dhuri, A. Gupta, S.M. Chaudhari, D.M. Phase, D.K. Avasthi, *Nucl. Instrum. Methods B* 156 (1999) 148.
- [17] M. Toulemonde, Ch. Dufour, E. Paumier, *Phys. Rev. B* 46 (1992) 14362.
- [18] D. Lesueur, A. Dunlop, *Radiat. Eff. Def. Solids* 126 (1993) 163.
- [19] A. Gupta, D.K. Avasthi, *Phys. Rev. B* 64 (2001) 155407.
- [20] S. Bagchi, S.R. Potdar, F. Singh, N.P. Lalla, *J. Appl. Phys.* 102 (2007) 074310.
- [21] S. Bagchi, N.P. Lalla, *J. Phys.: Condens. Matter* 20 (2008) 235202.
- [22] S. Bagchi, N.P. Lalla, *Thin Solid Films* 515 (2007) 5227.
- [23] L.G. Parratt, *Phys. Rev.* 95 (1954) 359.
- [24] Z.G. Wang, E. Ch Dufourtt, M. Paumierrt, Toulemonde, *J. Phys.: Condens. Matter* 6 (1994) 6733.
- [25] J.F. Ziegler, M.D. Ziegler, J.P. Biersack, *The Stopping and Range of Ions in Solids*, Pergamon, New York, 1985 <http://www.srim.org/SRIM/SRIM2006.htm>.
- [26] A. Audouard, E. Balanzat, S. Bouffard, C. Jousset, J.C. Chamberod, A. Dunlop, D.L. esueur, G. Fuchs, R. Spohr, J. Vetter, L. Thome, *Phys. Rev. Lett.* 65 (1990) 875.
- [27] A. Barbu, A. Dunlop, D. Lesueur, S. Averbach, *Europhys. Lett.* 15 (1991) 37.
- [28] Z.G. Wang, C. Dufour, E. Paumier, M. Toulemonde, *J. Phys.:Condens. Matter* 6 (1994) 6733.
- [29] A. Gupta, R.S. Chauhan, D.C. Agarwal, S. Kumar, S.A. Khan, A. Tripathi, D. Kabiraj, S. Mohapatra, T. Som, D.K. Avasthi, *J. Phys. D: Appl. Phys.* 41 (2008) 215306.
- [30] Z.A.R. Miedema, *Philips Tech. Rev.* 36 (1976) 217.
- [31] R. Dubey, A. Gupta, *J. Appl. Phys.* 98 (2005) 083903.
- [32] D. Weller, L. Folks, M. Best, E.E. Fullerton, B.D. Terris, G.J. Kusinski, K.M. Krishnan, G. Thomas, *J. Appl. Phys.* 89 (2001) 7525.
- [33] D. Aurongzeb, K.B. Ram, L. Menon, *Appl. Phys. Lett.* 87 (2005) 172509.
- [34] A. Paul, A. Gupta, P. Shah, K. Kawaguchi, G. Principi, *Hyperfine Interact.* 139 (2002) 205.
- [35] R. Shan, T.R. Gao, S.M. Zhou, X.S. Wu, Y.K. Fang, B.S. Han, *J. Appl. Phys.* 99 (2006) 063907.